J. Am. Chem. Soc. **1993,** *115,* 8187–8196

Allylidene Complexes from Tungsten Alkylidynes and Allyl Bromides: Structural Comparison and Dynamic Behavior†

Andreas Mayr,*[1] Marianna F. Asaro,[2,3] Timothy J. Glines,[2] Donna Van Engen,[2] and Gordon M. Tripp[1]

Contribution from the Departments of Chemistry, State University of New York at Stony Brook, Stony Brook, New York 11794-3400, and Princeton University, Princeton, New Jersey 08544

Received January 11, 1993

Abstract: The complexes [W(CPhCHCHR)$Br_2(CO)_2(NC_5H_4Me$-4)], **2a** (R = H) and **2b** (R = Me), and [W(CPhCHCHMe)$Br_2(CO)_2(NC_5H_4NMe_2$-4)], **2c**, were prepared by reaction of [W(CPh)Br$(CO)_2(NC_5H_4Me$-4$)_2$] and [W(CPh)Br$(CO)_2(NC_5H_4NMe_2$-4$)_2$] with allyl or 2-methylallyl bromide in 18–50% yield. The solid-state structures of all three compounds were determined by X-ray crystallography. Crystal data for **2a**: Space group $P2_1$, $a = 7.549(3)$ Å, $b = 12.648(5)$ Å, $c = 9.931(4)$ Å, $\beta = 90.65(3)°$, $Z = 2$, 1746 unique observed data, $F > 3\sigma(F)$, $R = 0.036$, $R_w = 0.037$. Crystal data for **2b**: Space group $P2_1/c$, $a = 8.352(2)$ Å, $b = 14.529(4)$ Å, $c = 18.209(6)$ Å, $\beta = 111.45(2)°$, $Z = 4$, 4048 unique observed data, $F > 3\sigma(F)$, $R = 0.051$, $R_w = 0.039$. Crystal data for **2c**: Space group $P\bar{1}$ (No. 2), $a = 7.109(2)$ Å, $b = 10.816(7)$ Å, $c = 14.942(5)$ Å, $\alpha = 76.62(4)°$, $\beta = 88.20(3)°$, $\gamma = 71.01(3)°$, $Z = 2$, 3123 unique observed data, $I > 3\sigma$, $R = 0.044$, $R_w = 0.039$. All three complexes displayed fluxional behavior in their variable-temperature NMR spectra. The detailed molecular motions associated with the solution dynamic processes are deduced from a comparison of the solid-state structures.

Introduction

The reactivity of Fischer-type carbyne, or alkylidyne, metal complexes toward organic substrates is still very little investigated.[4,5] Reactions of tungsten alkylidene complexes with alkenes were found to give stable metal alkylidyne alkene complexes.[6] Due to the stable bonding situation in such compounds, carbon–carbon bond formation between alkylidyne and alkene ligands is not expected to occur easily.[6] In this paper, we report the formation of three allylidene complexes from tungsten alkylidynes and allyl halides.[7,8] These reactions demonstrate that the inherent limitations for bond formation between alkylidyne ligands and alkenes may be overcome by using alkenes bearing suitable functional groups.

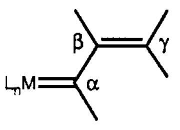

η^1-allylidene
(η^1-vinylcarbene)

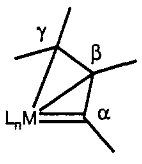

η^3-allylidene
(η^3-vinylcarbene)

Allylidene, or vinylcarbene, metal complexes have attracted considerable interest in recent years as postulated or demonstrated intermediates in stoichiometric and catalytic reactions, for example, in the formation of naphthols and other organic products from (carbene)carbonylchromium complexes and alkynes (Dötz reaction),[9,10] in alkyne polymerization,[11] in the formation of vinylketene metal complexes,[12] and in related processes.[13] A number of stable allylidene metal complexes have been prepared and characterized.[14,15] The allylidene fragment, $CRCRCR_2$, is capable of coordinating to transition metal centers in a variety of ways. Two major categories are (η^1- and (η^3-allylidene)metal complexes. The full range of coordination modes was recently investigated by Hofmann and co-workers using molecular orbital methods.[16] This theoretical study suggests that η^3-allylidene complexes are key intermediates in the Dötz reaction. According to these calculations, the allylidene complexes described in this work are similar in their electronic properties to the (unobservable) intermediates in the Dötz reaction. The three allylidene complexes investigated in this study differ selectively in their steric and electronic properties. As a result of the modifications, the allylidene ligands are found in three distinct bonding situations in the solid-state structures. The comparison of these structures

---

† Dedicated to Professor Herbert D. Kaesz on the occasion of his 60th birthday.

(1) State University of New York at Stony Brook.

(2) Princeton University.

(3) Present address: SRI International, Menlo Park, CA 94025.

(4) (a) Fischer, H.; Hofmann, P.; Kreissl, F. R.; Schrock, R. R.; Schubert, U.; Weiss, K. *Carbyne Complexes*; VCH Publishers: Weinheim, Germany, 1988. (b) Kim, H. P.; Angelici, R. J. *Adv. Organomet. Chem.* **1987**, *27*, 51. (c) Mayr, A.; Hoffmeister, H. *Adv. Organomet. Chem.* **1991**, *32*, 227.

(5) Mayr, A. *Comments Inorg. Chem.* **1990**, *10*, 227.

(6) (a) Mayr, A.; Dorries, A. M.; McDermott, G. A.; Geib, S. J.; Rheingold, A. L. *J. Am. Chem. Soc.* **1985**, *107*, 7775. (b) Mayr, A.; Dorries, A. M.; Rheingold, A. L.; Geib, S. J. *Organometallics* **1990**, *9*, 964.

(7) Mayr, A.; Asaro, M. F.; Glines, T. J. *J. Am. Chem. Soc.* **1987**, *109*, 2215.

(8) Mayr, A.; Asaro, M. F.; Van Engen, D. *NATO ASI Ser., Ser. C, 269* (*Adv. Met. Carbene Chem.*) **1989**, 167.

(9) (a) Dötz, K. H. *Angew. Chem.* **1975**, *87*, 672; *Angew. Chem., Int. Ed. Engl.* **1975**, *14*, 644. (b) Dötz, K. H. *Pure Appl. Chem.* **1983**, *55*, 1689.

(10) For example, see: (a) Dötz, K. H. *Angew. Chem.* **1984**, *96*, 573; *Angew. Chem., Int. Ed. Eng.* **1984**, *23*, 587–608. (b) Wulff, W. D.; Tang, P.-C.; Chan, K.-S.; McCallumn, J. S.; Yang, D. C.; Gilbertson, S. R. *Tetrahedron* **1985**, *41*, 5813. (c) Dötz, K. H. In *Organometallics in Organic Synthesis*; de Meijere, A., tom Diek, H., Eds.; Springer: New York, 1987. (d) Wulff, W. D. In *Advances in Metal-Organic Chemistry*; Liebeskind, L. S., Ed.; JAI Press Inc.: Greenwich, CT, 1989; Vol. 1. (e) Bos, M. E.; Wulff, W. D.; Miller, R. A.; Chamberlin, S.; Brandvold, T. A. *J. Am. Chem. Soc.* **1991**, *113*, 9293 and references herein.

(11) For example, see: (a) Katz, T. J.; Lee, S. J. *J. Am. Chem. Soc.* **1980**, *102*, 422. (b) Masuda, T.; Higashimura, T. *Adv. Polym. Sci.* **1986**, *81*, 121. (c) Feldman, J.; Schrock, R. R. *Prog. Inorg. Chem.* **1991**, *39*, 1.

(12) For example, see: (a) Jens, K.-J.; Weiss, E. *Chem. Ber.* **1984**, *117*, 2469. (b) Templeton, J. L.; Herrick, R. S.; Rusik, C. A.; McKenna, C. E.; McDonald, J. W.; Newton, W. E. *Inorg. Chem.* **1985**, *24*, 1383. (c) Green, M.; Orpen, A. G.; Schaverien, C. J.; Williams, I. D. *J. Chem. Soc., Dalton Trans.* **1985**, 2483. (d) Mitsudo, T.; Ishihara, A.; Kadokura, M.; Watanabe, Y. *Organometallics* **1986**, *5*, 238.

(13) For example, see: (a) Dötz, K. H.; Fügen-Köster, B. *Chem. Ber.* **1980**, *113*, 1449. (b) Yamashita, A.; Scahill, T. A. *Tetrahedron Lett.* **1982**, *23*, 3765. (c) Parlier, A.; Rudler, H.; Platzer, N.; Fontanille, M.; Soum, A. *J. Organomet. Chem.* **1985**, *287*, C8. (d) Wulff, W. D.; Gilbertson, S. R.; Springer, J. P. *J. Am. Chem. Soc.* **1986**, *108*, 520. (e) Garrett, K. E.; Feng, C. W.; Matsuzuka, H.; Geoffroy, G. L.; Rheingold, A. L. *J. Organomet. Chem.* **1990**, *394*, 251.

0002-7863/93/1515-8187$04.00/0

provides insight into the bonding of the allylidene complexes and forms the basis for an unusually detailed description of their solution dynamic behavior, which was revealed by variable-temperature NMR spectroscopy.

Results

Synthesis and Characterization of the Tungsten Allylidene Complexes. The tungsten alkylidyne complex **1a** reacts with excess allyl bromide in CH_2Cl_2 to afford the allylidene complex **2a** (eq 1).[7] No other carbonyl-containing product is formed as judged by IR. Complex **2a** is isolated in the form of dark brown crystals in about 50% yield after chromatography (silica gel/CH_2Cl_2) and recrystallization from CH_2Cl_2/pentane. Complex **2a** is stable in the solid state. In the absence of air, solutions of **2a** show no signs of decomposition for at least several hours. Complex **2b** is prepared analogously by reaction of **1a** with 2-methylallyl bromide.[8] Pure crystalline **2b** is isolated in 18% yield by repeated chromatography and slow crystallization from CH_2Cl_2/ether. Complex **2b** is less stable than **2a**, showing signs of decomposition upon standing in solution, even under nitrogen. Complex **2c**, containing a 4-(dimethylamino)pyridine ligand instead of the 4-picoline ligand, is prepared in the same way as **2a** from the alkylidyne complex **1b** and allyl bromide and is isolated in 28% yield. The stability of **2c** appears to be similar to that of **2a**.

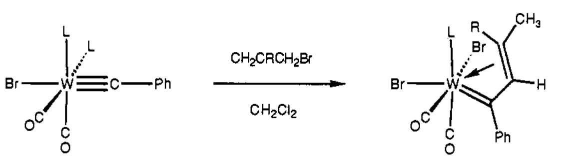

(1)

1a: L = 4-picoline
1b: L = 4-dimethylaminopyridine

2a: L = 4-picoline, R = H
2b: L = 4-picoline, R = CH_3
2c: L = 4-dimethylaminopyridine, R = H

Spectroscopic Studies. All three complexes exhibit two IR absorptions in the metal carbonyl region. Complexes **2a,c** exhibit a sharp band of medium intensity near 2025 cm^{-1} and a strong broad band near 1940 cm^{-1}. The corresponding absorptions for **2b** are at 2007 and 1923 cm^{-1}. The ^1H-NMR spectrum of **2a** shows the presence of one picoline ligand, a phenyl group, and a methylvinyl group. A portion of the room-temperature ^1H NMR spectrum of **2a** is shown as the upper trace in Figure 1. The methyl substituent of the vinyl group gives rise to a doublet at δ 1.86. The vinyl hydrogen atoms appear as a multiplet at δ 5.61 (CHMe) and a doublet at δ 5.29 (CH). A resonance at δ 240.4 in the ^{13}C-NMR spectrum is assigned to the alkylidene carbon atom. Resonances at δ 210.8 and 209.8 show the presence of two carbonyl ligands. Signals at δ 122.9 and 91.3 are assigned to the vinyl CHMe and CH carbon atoms, respectively.[17,18] The dimethylvinyl group of **2b** gives rise to three signals in the ^1H NMR spectrum, a broad peak at δ 5.65 for the vinyl hydrogen atom and a sharp signal at δ 1.81 as well as a broad signal at δ 1.62 for the two methyl groups. The broadness of some of the signals is indicative of dynamic behavior (see below). The ^{13}C NMR spectrum of **2b** shows signals for the alkylidene carbon at δ 230 and for the carbonyl ligands at δ 213.9 and 212.6 and the expected number of signals for the aromatic carbon atoms as well as for the methyl groups. A broad signal at δ 91.9 is assigned to the hydrogen-substituted vinyl carbon atom, CH. The resonance for the dimethyl-substituted vinyl carbon atom, CMe_2, could not be detected in the room-temperature ^{13}C NMR spectrum. At lower temperatures, however, two singlets at δ 204.8 and 194.5 can be assigned to the CMe_2 carbon atom of two conformational isomers. The NMR data for **2c** are very similar to those for **2a**.

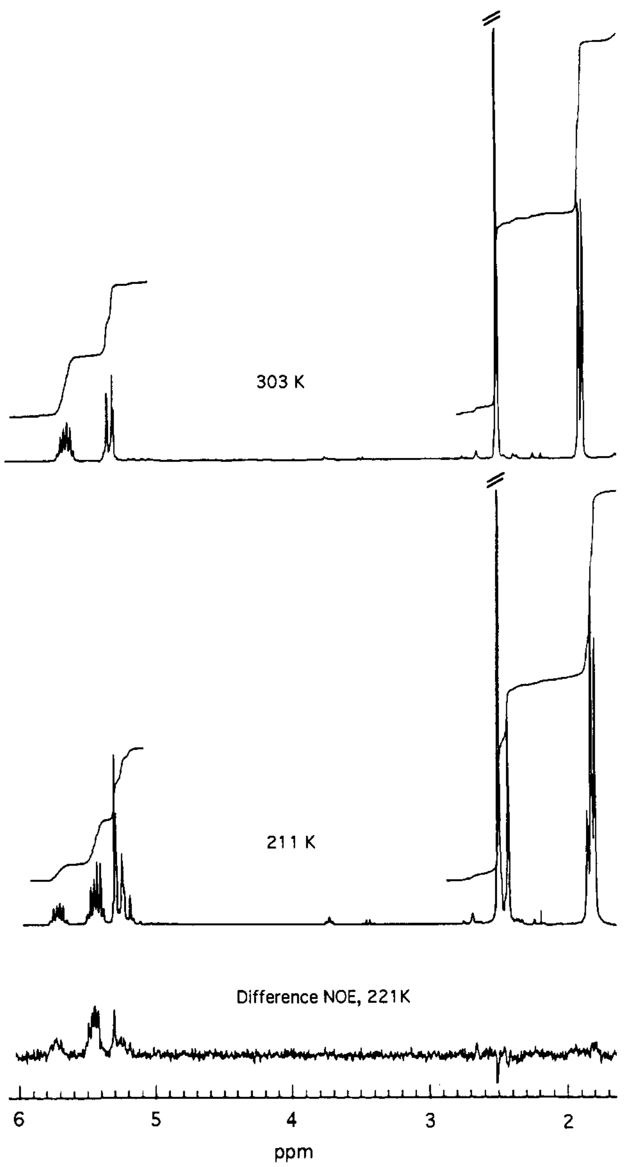

Figure 1. Partial ^1H NMR spectra of **2a** at 303 K (top) and at 211 K (middle) and difference NOE spectrum of **2a** at 221 K with irradiation at resonance frequency of picoline α-hydrogen atoms (lower trace).

---

(14) (a) Mitsudo, T.; Nakanishi, H.; Inubishi, T.; Morishima, I.; Watanabe, Y.; Takegami, Y. *J. Chem. Soc., Chem. Commun.* **1976**, 416. (b) Nakatsu, K.; Mitsudo, T.; Nakanishi, H.; Watanabe, Y.; Takegami, Y. *Chem. Lett.* **1977**, 1447. (c) Mitsudo, T.; Nakanishi, H.; Inubishi, T.; Morishima, I.; Watanabe, Y.; Takegami, Y. *J. Chem. Soc., Dalton Trans.* **1978**, 1298. (d) Klimes, J.; Weiss, E. *Angew. Chem.* **1982**, *94*, 207; *Angew. Chem., Int. Ed. Engl.* **1982**, *21*, 205. (e) Morrow, J. R.; Tonker, T. L.; Templeton, J. L. *J. Am. Chem. Soc.* **1985**, *107*, 5004. (f) Herrmann, W. A.; Fischer, R. A.; Herdtweck, E. *Angew. Chem.* **1987**, *99*, 1286; *Ang. Chem., Int. Ed. Engl.* **1987**, *26*, 1263. (g) Valérie, T.; Meier, F.; Weiss, E. *Chem. Ber.* **1988**, *121*, 1093. (h) Herrmann, W. A.; Fischer, R. A.; Felixberger, J. K.; Paciello, R. A.; Kiprof, P.; Herdtweck, E. *Z. Naturforsch. B* **1988**, *43*, 1391. (i) Fischer, R. A.; Fischer, R. W.; Herrmann, W. A.; Herdtweck, E. *Chem. Ber.* **1989**, *122*, 2035. (j) Garrett, K. E.; Sheridan, J. B.; Poureau, D. B.; Feng, W. C.; Geoffroy, G. L.; Staley, D. L.; Rheingold, A. L. *J. Am. Chem. Soc.* **1989**, *111*, 8383.

(15) (a) McCullough, L. G.; Listemann, M. L.; Schrock, R. R.; Churchill, M. R.; Ziller, J. W. *J. Am. Chem. Soc.* **1983**, *105*, 6729. (b) Parlier, A.; Rudler, M.; Rudler, H.; Daran, J. C. *J. Organomet. Chem.* **1987**, *323*, 353. (c) Binger, P.; Müller, P.; Benn, R.; Mynott, R. *Angew. Chem.* **1989**, *101*, 647; *Angew. Chem., Int. Ed. Engl.* **1989**, *28*, 610. (d) Le Bozec, H.; Ouzzine, K.; Dixneuf, P. *J. Chem. Soc., Chem. Commun.* **1989**, 219. (e) Wallace, K. C.; Liu, A. H.; Davis, W. M.; Schrock, R. R. *Organometallics* **1989**, *8*, 644. (f) Feng, S. G.; Gamble, A. S.; Templeton, J. L. *Organometallics* **1989**, *8*, 2024. (g) Fischer, H.; Hofmann, J.; Mauz, E. *Angew. Chem.* **1991**, *103*, 1013; *Angew. Chem., Int. Ed. Engl.* **1991**, *30*, 998.

(16) (a) Hofmann, P.; Hämmerle, M. *Angew. Chem.* **1989**, *101*, 940; *Angew. Chem., Int. Ed. Engl.* **1989**, *28*, 908. (b) Hofmann, P.; Hämmerle, M.; Unfried, G. *New J. Chem.* **1991**, *15*, 769.

(17) The assignments of the ^{13}C NMR peaks of the vinyl group are based on an observed broadening of the signal at δ 91.3 for the ^{13}C-labeled complex $W(C^*PhCHCHMe)Br_2(C^*O)_2(pic)$.[18]

(18) Asaro, M. F.; Mayr, A. Manuscript in preparation.

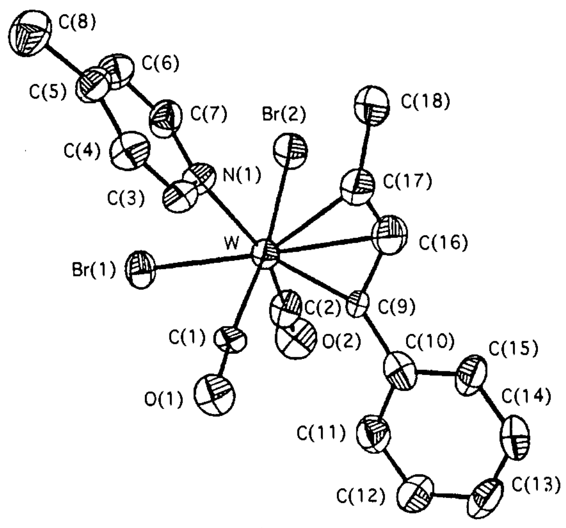

Figure 2. Molecular structure of **2a**.

The ^{1}H NMR resonances of **2a–c** broaden upon cooling, and at low temperatures two sets of similar spectra are obtained for each of the three compounds. Figure 1 shows a portion of the ^{1}H NMR spectrum of complex **2a** at 211 K (middle trace of Figure 1). At low temperatures two isomers, I and II, are observed for **2a,c** in a relative ratio of about 2:1. In the low-temperature spectra of both **2a,c**, the pyridine α-hydrogen atoms of the more abundant isomers I give rise to two signals, i.e. the corresponding isomers of **2a,c** appear to have the same relative stabilities. The low-temperature signal sets of compound **2b** are present at a relative ratio of almost exactly 1:1. On the basis of an estimated coalescence temperature of 278 K for the vinyl CH signals, the free energy of activation for the dynamic process of complex **2b** was calculated to be $\Delta G^{\ddagger} = 54$ kJ/mol.[19] The free energy of activation for the dynamic process of **2a** (I → II) was obtained as $\Delta G^{\ddagger} = 47$ kJ/mol, on the basis of an estimated coalescence temperature of 253 K of the CHMe signals.[19b]

The spacial arrangement of the ligands in complex **2a** was probed by difference NOE experiments. Irradiation of a sample of complex **2a** at the frequency of the picoline α-hydrogen atoms leads to a significant enhancement of the signals of the vinyl hydrogen atom C(17)HMe (lower trace in Figure 1; for the numbering of the atoms, see Figure 2). The signal of the vinyl hydrogen atom C(16)H is only slightly enhanced. A very small NOE is observed for the signal of the methyl hydrogen atoms C(18)H_3. The NOE correlation between the picoline α-hydrogen atoms and C(17)H was confirmed by the observation of an enhanced signal for the picoline α-H atoms upon irradiation at the resonance frequency of C(17)H.

Solid-State Structure of Complex 2a. The molecular structure of **2a** is shown in Figure 2. Crystal data are collected in Table I. Final atomic positional parameters are shown in Table II; selected bond distances and bond angles are listed in Table V. The coordination geometry could be considered distorted octahedral, with the allylidene ligand occupying one coordination site. However, as will be discussed further below, in complexes **2** the allylidene ligand may be segmented into tow components, namely a carbene and a vinyl group. On this basis, the coordination geometry is considered distorted monocapped trigonal prismatic, whereby the carbene carbon and the vinyl group define the edge of the trigonal prism opposite to the capping site, which is occupied by Br(1). The metal allylidene, or vinylcarbene, fragment is obviously the structural feature of greatest interest. The distance between tungsten and the alkylidene carbon, W–C(9) = 1.98(2) Å, is typical of a tungsten–carbon double bond.[20] The distances between tungsten and the vinyl carbon atoms, W–C(16) = 2.38(2) and W–C(17) = 2.60(2) Å, are very long for a coordinated carbon–carbon double bond[21] and even long for an allyl-type ligand.[22] The length of the bond connecting the alkyidene carbon and the vinyl group, C(9)–C(16), is 1.44(2) Å. This distance is close to the value expected for a single bond between two sp^2 carbon centers.[23] The C(16)–C(17) distance of 1.35(1) Å is very close to the standard carbon–carbon double bond length of free olefins.[23] Thus the tungsten–carbon and the carbon–carbon double bonds are largely localized. The possibility of conjugation between these double bond systems is strongly reduced due to rotation of the vinyl group out of the plane of the alkylidene ligand as measured by the dihedral angle W–C(9)–C(16)–C(17), which is 54.4(2)°. The two bond angles around the alkylidene carbon atom which involve the metal center are strongly distorted, W–C(9)–C(10) = 149(1)° and W–C(9)–C(16) = 87.1(9)°. The third angle, C(10)–C(9)–C(16) = 124(2)°, is normal. The intraligand angles C(9)–C(16)–C(17) = 122(2)° and C(16)–C(17)–C(18) = 127(2)° are essentially normal. The two carbonyl ligands and the picoline ligand are bent toward the capping site: Br(1)–W–C(1) = 79.1(4)°, Br(1)–W–C(2) = 77.6(4)°, and Br(1)–W–N(1) = 81.3(3)°. The angle between the two bromide ligands is somewhat larger: Br(1)–W–Br(2) = 91.5(1)°. These bonding angles are in the same range as those found in other monocapped trigonal prismatic structures.[24]

Solid-State Structure of Complex 2b. The molecular structure of complex **2b** is shown in Figure 3. Crystal data are collected in Table I. Final atomic positional parameters are shown in Table III; selected bond distances and bond angles are listed in Table VI. The distance between tungsten and the alkylidene carbon C(1) is 1.951(8) Å. The vinyl carbon atoms are unusually distant from the metal center, W–C(2) = 2.440(11) Å and W–C(3) = 3.158(8) Å. The latter distance is too long to be considered within bonding range. The intraligand bond lengths C(1)–C(2) and C(2)–C(3) of 1.49(2) and 1.34(2) Å, respectively, almost coincide with standard values for single and double bonds between sp^2 carbon centers.[20] Thus the tungsten–carbon and the carbon–carbon double bonds are localized. There is, in fact, no delocalization possible between these double bond systems as they are oriented almost exactly perpendicular relative to each other. The dihedral angle W–C(1)–C(2)–C(3) is 91.8(8)°. The bond angles of the alkylidene carbon involving the metal center are strongly distorted, W–C(1)–C(2) = 89.3(5)° and W–C(1)–C(6) = 148.0(9)°. The third angle, C(2)–C(1)–C(6) = 122.6(9)°, is normal. The angle C(1)–C(2)–C(3) is 121.9(9)°. The bond angles around the terminal vinyl carbon atom, C(2)–C(3)–C(4) = 125.7(10)°, C(2)–C(3)–C(5) = 118.3(9)°, and C(4)–C(3)–C(5) = 115.7(9)°, add up to 359.7°; i.e., the vinyl carbon atom C(3) is planar. The dihedral angle C(1)–C(2)–C(3)–C(5) of 176.2(8)° indicates that the entire vinyl group is essentially planar. The two carbonyl ligands and the picoline ligand are bent toward the capping ligand Br(2): Br(2)–W–C(19) = 78.0(3)°, Br(2)–W–C(20) = 80.9(3)°, and Br(2)–W–N(12) = 85.8(2)°. The Br(1)–W–Br(2) bond angle is 91.3(1)°.

Solid-State Structure of Complex 2c. The molecular structure of **2c** is shown in Figure 4. Crystal data are collected in Table

---

(19) (a) Sandström, J. *Dynamic NMR Spectroscopy*; Academic Press: London, 1982. (b) Shanan-Atidi, H.; Bar-Eli, K. H. *J. Phys. Chem.* **1970**, *74*, 961. Due to considerable uncertainties in the assessments of the coalescence temperatures, only the magnitude, not the precise values, of the calculated free energies of activation should be considered significant.

(20) (a) Mayr, A.; Lee, K. S.; Kjelsberg, M. A.; Van Engen, D. *J. Am. Chem. Soc.* **1986**, *108*, 6079. (b) Churchill, M. R.; Youngs, W. J. *Inorg. Chem.* **1979**, *18*, 2454.

(21) (a) Sharp, P. R. *Organometallics* **1984**, *3*, 1217. (b) Mayr, A.; Dorries, A. M.; Rheingold, A. L.; Geib, S. J. *Organometallics* **1990**, *9*, 964.

(22) (a) Huttner, G.; Brintzinger, H. H.; Bell, L. G.; Friedrich, P.; Bejenke, V.; Neugebauer, D. *J. Organomet. Chem.* **1978**, *145*, 329. (b) Greenbough, T. J.; Legzdins, P.; Martin, D. T.; Trotter, J. *Inorg. Chem.* **1979**, *18*, 3268.

(23) *Tables of Interatomic Distances and Configuration of Molecules and Ions*; Sutton, L. E., Ed.; The Chemical Society: London, 1965.

(24) (a) LaRue, W. A.; Liu, A. T.; Filippo, J. S. *Inorg. Chem.* **1980**, *19*, 315. (b) Lewis, D. F.; Lippard, S. J. *Inorg. Chem.* **1972**, *11*, 621.

Table I. Crystallographic Data for Complexes **2a–c**

	2a	**2b**	**2c**
	(a) Crystal Parameters		
formula	$C_{18}H_{17}Br_2NO_2W$	$C_{19}H_{19}Br_2NO_2W$	$C_{19}H_{20}Br_2N_2O_2W$
space group	$P2_1$	$P2_1/c$	$P\bar{1}$
a, Å	7.549(3)	8.352(2)	7.109(2)
b, Å	12.648(5)	14.529(4)	10.816(7)
c, Å	9.931(4)	18.209(6)	14.942(5)
α, deg			76.62(4)
β, deg	90.65(3)	111.45(2)	88.20(3)
γ, deg			71.01(3)
V, Å^3	948.2(6)	2056(1)	1055.4(9)
Z	2	4	2
D(calcd), g cm^{-3}	2.18	2.06	2.051
color	dark brown	black	dark brown
size, mm	0.16 × 0.20 × 0.23	0.15 × 0.25 × 0.35	0.3 × 0.3 × 0.1
	(b) Data Collection and Refinement		
diffractometer	Nicolet R3m	Nicolet R3m	Enraf-Nonius CAD4
temp, °C	−93	ambient	ambient
radiation	Mo Kα	Mo Kα	Mo Kα
monochromator	graphite single crystal	graphite single crystal	graphite single crystal
scan limits, deg	$3 < 2\theta < 50$	$3 < 2\theta < 52$	$0 < 2\theta < 60.8$
no. of obsd reflcns	1663	2991	3123
no. of params	217	227	235
$R(F)$	0.036	0.051	0.044
$R_w(F)$	0.037	0.039	0.039
GOF	1.25	1.48	1.21

Table II. Final Atomic Coordinates (×10^4) and Isotropic Thermal Parameters (Å^2 × 10^3) of **2a**

	x	y	z	U^a
W	1358(1)	0	1099(1)	31(1)
Br(1)	−1549(2)	−1080(1)	1347(2)	42(1)
Br(2)	3099(2)	−1685(1)	358(2)	45(1)
C(1)	−281(16)	1108(11)	1728(12)	29(4)
O(1)	−1115(14)	1750(9)	2170(11)	48(3)
C(2)	1610(20)	−595(11)	2943(16)	41(5)
O(2)	1737(16)	−943(10)	3997(12)	58(4)
N(1)	285(13)	176(9)	−1044(10)	31(3)
C(3)	−396(19)	1090(14)	−1478(15)	40(5)
C(4)	−1179(19)	1228(13)	−2733(14)	39(4)
C(5)	−1407(19)	355(12)	−3569(14)	40(5)
C(6)	−741(23)	−589(13)	−3100(18)	45(5)
C(7)	89(21)	−651(13)	−1855(17)	44(5)
C(8)	−2390(23)	458(16)	−4902(16)	55(5)
C(9)	2936(15)	1032(12)	2004(12)	32(4)
C(10)	3344(18)	1669(14)	3182(16)	44(5)
C(11)	2341(21)	1614(15)	4385(16)	48(5)
C(12)	2816(22)	2214(14)	5474(17)	54(6)
C(13)	4211(23)	2905(15)	5421(18)	56(6)
C(14)	5201(20)	2990(14)	4232(17)	50(5)
C(15)	4732(20)	2375(13)	3151(17)	47(5)
C(16)	4154(22)	861(14)	926(18)	52(5)
C(17)	3655(21)	980(15)	−375(16)	52(6)
C(18)	4572(22)	594(16)	−1567(18)	62(6)

^{a} Equivalent isotropic U defined as one-third of the trace of the orthogonalized $\mathbf{U}_{ij}$ tensor.

Table III. Final Atomic Coordinates (×10^4) and Isotropic Thermal Parameters (Å^2 × 10^3) of **2b**

	x	y	z	U^a
W	1898(1)	2375(1)	3054(1)	49(1)
Br(1)	2503(2)	909(1)	2353(1)	73(1)
Br(2)	−1011(2)	1707(1)	3003(1)	73(1)
C(1)	4063(12)	2989(6)	3650(5)	54(4)
C(2)	4549(12)	2943(6)	2942(5)	57(4)
C(3)	4186(11)	3629(6)	2411(5)	55(4)
C(4)	3339(13)	4516(6)	2462(6)	70(5)
C(5)	4815(14)	3552(8)	1750(6)	76(5)
C(6)	5207(13)	3367(6)	4403(5)	55(4)
C(7)	6760(14)	3759(7)	4450(7)	71(5)
C(8)	7890(16)	4115(8)	5164(7)	85(6)
C(9)	7443(16)	4090(8)	5818(7)	88(6)
C(10)	5910(15)	3734(7)	5774(6)	82(5)
C(11)	4769(14)	3366(7)	5063(6)	70(5)
N(12)	384(9)	2966(5)	1837(4)	49(3)
C(13)	−817(11)	3628(6)	1760(5)	57(4)
C(14)	−1713(12)	4034(7)	1051(5)	63(4)
C(15)	−1473(13)	3768(7)	374(6)	64(4)
C(16)	−240(14)	3091(7)	458(6)	69(5)
C(17)	609(13)	2714(7)	1178(6)	61(4)
C(18)	−2457(16)	4208(8)	−410(6)	90(6)
C(19)	1065(13)	3355(7)	3597(5)	57(4)
O(19)	590(10)	3889(5)	3923(4)	81(4)
C(20)	2718(14)	1657(6)	4042(6)	66(5)
O(20)	3194(11)	1239(5)	4612(4)	95(4)

^{a} Equivalent isotropic U defined as one-third of the trace of the orthogonalized $\mathbf{U}_{ij}$ tensor.

I. Final atomic positional parameters are shown in Table IV; selected bond distances and bond angles are listed in Table VII. The length of the tungsten–carbon double bond, W–C(9), is 1.96(1) Å. The distances between tungsten and the vinyl carbon atoms, W–C(16) and W–C(17), are 2.33(1) and 2.58(1) Å, respectively. The intraligand distances C(9)–C(16) and C(16)–C(17) are 1.48(1) and 1.28(1) Å, respectively.[25] The angle between the plane of the vinyl group and the plane of the alkylidene ligand, as measured by the dihedral angle W–C(9)–C(16)–C(17), is −61(1)°. The bond angles around the alkylidene carbon atom W–C(9)–C(10), W–C(9)–C(16), and C(10)–C(9)–C(16) are 147.9(7)°, 83.3(6)°, and 126.3(9)°, respectively. The two carbonyl ligands, the picoline ligand, and the bromide ligand are all bent toward the capping site: Br(1)–W–C(1) = 80.1(3)°, Br(1)–W–C(2) = 77.9(3)°, Br(1)–W–N(1) = 85.2(2)°, and Br(1)–W–Br(2) = 84.81(5)°.

Discussion

Formation of the Allylidene Ligands from Alkylidyne Ligands and Allyl Bromides. It is not known how the allylidene complexes form, but the qualitative observation that the reactions proceed at about the same rate as the substitution of pyridine ligands in complexes 1 suggests that coordination of the alkene portion of the allyl bromides to the metal center is the first step. The

---

[25] This carbon–carbon double-bond distance of 1.28(1) Å is unusually short. However, the sum of the C(9)–C(16), C(16)–C(17), and C(17)–C(18) bond lengths, 4.25 Å, is the same as the sum of the corresponding distances in **2a**. Similarly short carbon–carbon double-bond distances in stilbenes were shown to be artifacts of the structure solutions, being caused by disorder in the crystal. Ogawa, K.; Sano, T.; Yoshimura, S.; Takeuchi, Y.; Toriumi, K. *J. Am. Chem. Soc.* **1992**, *114*, 1041. A specific cause for the shortness of the C(16)–C(17) bond in **2c** could not be discerned.

Table IV. Final Atomic Positional Parameters and B(eq) Values (Å^2) of **2c**

atom	x	y	z	B(eq)
W(1)	0.02318(6)	0.23356(5)	−0.23930(3)	2.25(2)
Br(1)	−0.2109(2)	0.2756(1)	−0.38137(7)	3.96(8)
Br(2)	−0.1555(2)	0.0593(1)	−0.15923(8)	4.19(9)
O(1)	0.158(1)	0.4480(8)	−0.3749(5)	5.0(6)
O(2)	−0.373(1)	0.4408(8)	−0.1940(5)	5.1(6)
N(1)	0.231(1)	0.0737(7)	−0.2985(5)	2.3(5)
N(2)	0.643(1)	−0.224(1)	−0.4087(5)	4.2(7)
C(1)	0.111(1)	0.367(1)	−0.3265(7)	3.1(7)
C(2)	−0.225(1)	0.369(1)	−0.2116(6)	3.2(7)
C(3)	0.415(1)	0.081(1)	−0.3253(7)	3.3(7)
C(4)	0.551(1)	−0.012(1)	−0.3618(7)	3.4(7)
C(5)	0.512(1)	−0.125(1)	−0.3756(6)	3.3(7)
C(6)	0.321(1)	−0.132(1)	−0.3489(7)	3.9(8)
C(7)	0.193(1)	−0.032(1)	−0.3137(7)	3.7(8)
C(8)	0.598(2)	−0.338(1)	−0.4242(8)	5(1)
C(8A)	0.836(2)	−0.210(1)	−0.4394(8)	5(1)
C(9)	0.117(1)	0.326(1)	−0.1580(6)	2.8(6)
C(10)	0.111(1)	0.451(1)	−0.1370(6)	2.8(7)
C(11)	−0.017(2)	0.574(1)	−0.1858(7)	4.0(8)
C(12)	−0.026(2)	0.691(1)	−0.1616(8)	5(1)
C(13)	0.093(2)	0.686(1)	−0.0906(8)	5(1)
C(14)	0.221(2)	0.567(1)	−0.0433(8)	4(1)
C(15)	0.233(1)	0.449(1)	−0.0656(7)	3.6(8)
C(16)	0.281(2)	0.197(1)	−0.1336(7)	4.4(9)
C(17)	0.250(2)	0.086(1)	−0.0971(7)	4.5(9)
C(18)	0.387(1)	−0.054(1)	−0.0880(7)	3.9(8)

Table V. Selected Bond Distances and Bond Angles for **2a**

	(a) Bond Distances (Å)		
W–Br(1)	2.599(2)	W–Br(2)	2.614(2)
W–C(1)	1.98(2)	W–C(2)	1.99(2)
W–N(1)	2.28(1)	W–C(9)	1.98(2)
W–C(16)	2.38(2)	W–C(17)	2.60(2)
C(1)–O(1)	1.12(2)	C(2)–O(2)	1.14(2)
C(9)–C(16)	1.44(2)	C(16)–C(17)	1.35(1)
	(b) Bond Angles (deg)		
Br(1)–W–Br(2)	91.5(1)	Br(1)–W–C(1)	79.1(4)
Br(2)–W–C(1)	170.4(4)	Br(1)–W–C(2)	77.6(4)
Br(2)–W–C(2)	84.7(4)	C(1)–W–C(2)	91.8(6)
Br(1)–W–N(1)	81.3(3)	Br(2)–W–N(1)	89.5(3)
C(1)–W–N(1)	90.5(5)	C(2)–W–N(1)	157.9(5)
Br(1)–W–C(9)	144.0(4)	Br(2)–W–C(9)	111.3(4)
C(1)–W–C(9)	76.4(5)	C(2)–W–C(9)	77.3(6)
N(1)–W–C(9)	124.5(5)	W–C(1)–O(1)	174.(1)
W–C(2)–O(2)	179.2(7)	W–C(9)–C(10)	149.(1)
W–C(9)–C(16)	87.1(9)	C(10)–C(9)–C(16)	124.(2)
C(9)–C(16)–C(17)	122.(2)	C(16)–C(17)–C(18)	127.(2)

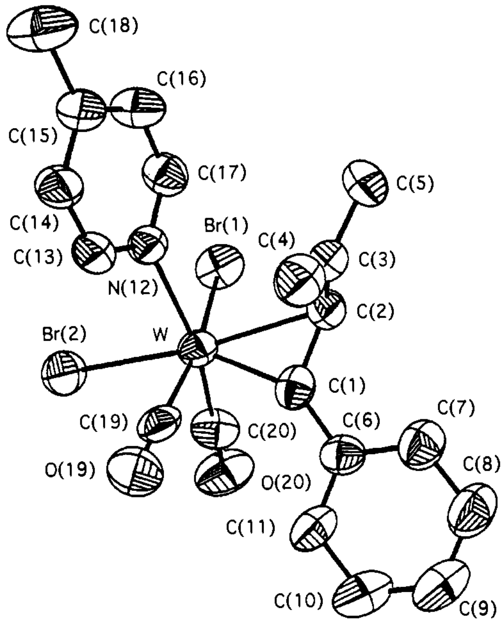

Figure 3. Molecular structure of **2b**.

Table VI. Selected Bond Distances and Bond Angles for **2b**

	(a) Bond Distances (Å)		
W–Br(1)	2.626(1)	W–Br(2)	2.587(1)
W–C(1)	1.951(8)	W–C(2)	2.440(11)
W–N(12)	2.279(6)	W–C(19)	1.999(11)
W–C(20)	1.973(10)	C(1)–C(2)	1.49(2)
C(1)–C(6)	1.46(2)	C(2)–C(3)	1.34(2)
C(3)–C(4)	1.49(2)	C(3)–C(5)	1.48(2)
C(19)–O(19)	1.13(2)	C(20)–O(20)	1.14(2)
	(b) Bond Angles (deg)		
Br(1)–W–Br(2)	91.3(1)	Br(1)–W–C(1)	109.7(3)
Br(2)–W–C(1)	149.2(3)	Br(1)–W–C(2)	83.8(2)
Br(2)–W–C(2)	173.2(2)	C(1)–W–C(2)	37.6(4)
Br(1)–W–N(12)	88.3(2)	Br(2)–W–N(12)	85.8(2)
C(1)–W–N(12)	116.1(3)	C(2)–W–N(12)	89.4(3)
Br(1)–W–C(19)	169.2(3)	Br(2)–W–C(19)	78.0(3)
C(1)–W–C(19)	79.6(4)	C(2)–W–C(19)	107.0(4)
N(12)–W–C(19)	92.4(3)	Br(1)–W–C(20)	87.1(3)
Br(2)–W–C(20)	80.9(3)	C(1)–W–C(20)	78.0(4)
C(2)–W–C(20)	103.4(4)	N(12)–W–C(20)	165.8(4)
C(19)–W–C(20)	89.6(4)	W–C(1)–C(2)	89.3(5)
W–C(1)–C(6)	148.0(9)	C(2)–C(1)–C(6)	122.6(9)
W–C(2)–C(1)	53.1(5)	W–C(2)–C(3)	109.8(6)
C(1)–C(2)–C(3)	121.9(9)	C(2)–C(3)–C(4)	125.7(10)
C(2)–C(3)–C(5)	118.3(9)	C(4)–C(3)–C(5)	115.7(9)
W–C(19)–O(19)	177.6(9)	W–C(20)–O(20)	179.8(9)

coordinated carbon–carbon double bond in intermediate **3** would be oriented perpendicular to the metal–carbon triple bond. The reactive halomethyl group then points either toward the alkylidyne ligand (**3a**) or toward the opposite side (**3b**). In intermediate **3a**, carbon–carbon bond formation could occur by direct electrophilic attack of the bromomethyl group at the alkylidyne carbon, followed by hydrogen migration to give the allylidene complexes **2**. In intermediate **3b**, the bromomethyl group could undergo oxidative addition to the metal center, causing the loss of the carbonyl ligands and giving rise to the unidentified carbonyl-free byproducts. The formation of several polycyclic organic products from metal alkylidyne complexes and enynes may also be considered as an example of carbon–carbon bond formation between an alkylidyne ligand and a functionalized alkene.[26]

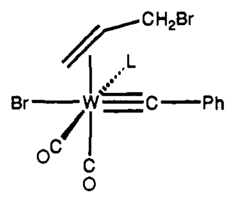

3a

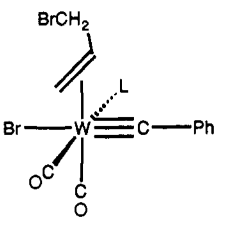

3b

Probing the Influence of Steric and Electronic Properties on the Bonding of Allylidene Ligands. Complex **2b** is formally derived from **2a** by introduction of an additional methyl group on the γ-carbon of the allylidene ligand. The additional methyl group, C(4)H$_3$, interferes sterically with the picoline ligand. The C(4)–N(12) distance is 3.23(2) Å, which corresponds well to the sum of the van der Waals radii of an sp^2-hybridized nitrogen atom and a methyl group.[20] Because of this steric interaction, the dimethyl-substituted vinyl group in **2b** cannot approach the metal center as closely as the methyl-substituted vinyl group in **2a**. In comparison to **2a**, the vinyl group in **2b** is rotated about the WC(Ph)–CHCMe$_2$ bond. The dihedral angle between the planes of

---

(26) Sivavec, T. M.; Katz, T. J.; Chiang, M. Y.; Yang, G. X.-Q. *Organometallics* **1989**, *8*, 1620.

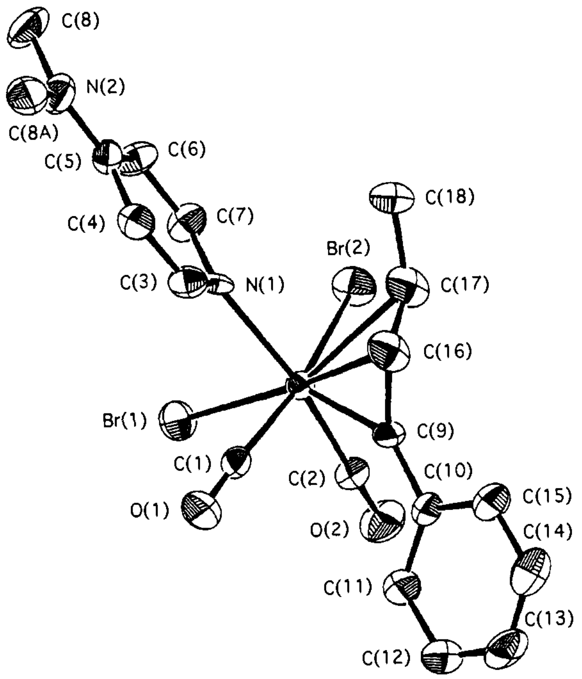

Figure 4. Molecular structure of **2c**.

Table VII. Selected Bond Distances and Bond Angles for **2c**

(a) Bond Distances (Å)

W–Br(1)	2.601(1)	W–Br(2)	2.649(2)
W–C(1)	1.96(1)	W–C(2)	2.00(1)
W–N(1)	2.218(7)	W–C(9)	1.987(9)
W–C(16)	2.33(1)	W–C(17)	2.58(1)
C(1)–O(1)	1.13(1)	C(2)–O(2)	1.15(1)
C(9)–C(10)	1.45(1)	C(9)–C(16)	1.48(1)
C(16)–C(17)	1.28(1)	C(17)–C(18)	1.49(2)

(b) Bond Angles (deg)

Br(1)–W–Br(2)	84.81(5)	Br(1)–W–C(1)	80.1(3)
Br(2)–W–C(1)	164.9(3)	Br(1)–W–C(2)	77.9(3)
Br(2)–W–C(2)	83.6(3)	C(1)–W–C(2)	94.1(4)
Br(1)–W–N(1)	85.2(2)	Br(2)–W–N(1)	88.8(2)
C(1)–W–N(1)	89.0(3)	C(2)–W–N(1)	162.0(3)
Br(1)–W–C(9)	143.3(3)	Br(2)–W–C(9)	116.7(3)
C(1)–W–C(9)	76.9(4)	C(2)–W–C(9)	75.6(4)
N(1)–W–C(9)	122.3(3)	W–C(1)–O(1)	177.1(8)
W–C(2)–O(2)	175.6(9)	W–C(9)–C(10)	147.9(7)
W–C(9)–C(16)	83.3(6)	C(10)–C(9)–C(16)	126.3(9)
C(9)–C(16)–C(17)	122(1)	C(16)–C(17)–C(18)	129(1)

the MC and CC double bonds is wider by 37.4° in **2b** than it is in **2a**. The steric repulsion between the vinyl group and the picoline ligand in **2b** is accommodated almost exclusively by this movement of the vinyl group. The picoline ligand in **2b** is not pushed toward the capping bromide ligand. On the contrary, the picoline ligand even relaxes toward the vinyl group. The coordination angle between the picoline and the capping bromide (N(1)–W–Br(1) in **2a**) is wider by 3.9° in **2b** than it is in **2a**. The structural changes associated with the introduction of the additional methyl group are clearly visible in the superimposition of structures **2a** and **2b** shown in Figure 5.

To selectively probe the influence of electronic effects on the bonding of the allylidene ligand, we sought to change the electron density of the metal center without introducing significant changes in the steric environment. Complex **2c** contains a 4-(dimethylamino)pyridine ligand instead of the 4-picoline ligand in **2a**. These two ligands have essentially identical steric properties in the vicinity of the metal center, but the 4-(dimethylamino)pyridine is a slightly stronger donor ligand as indicated by a comparison of the carbonyl stretching frequencies of **1a** (1987, 1898 cm^{-1}) and **1b** (1979, 1887 cm^{-1}). Due to the weakness of the metal–vinyl interaction, which is evident from the structures of complexes **2a**,**b**, we anticipated a noticeable structural influence even due to a small increase of the electron density of the metal center. The structural differences between **2a** and **2c** turned out to be more dramatic than expected. In complexes **2a**,**c** opposite sides of the vinyl group are facing the metal center, but the structures do not reveal any distinctive influence of the small change in electron density of the metal centers on the intrinsic bonding of the allylidene ligand. Nevertheless, the result obtained is highly informative regarding the dynamic behavior of the allylidene complexes in solution. Structures **2a**,**c**, in which the vinyl groups are "turned around", represent the two isomers (diastereomers) which are postulated to interconvert on the NMR time scale. The NMR data show that the corresponding conformational isomers of **2a**,**c** have almost identical relative energies. Therefore, we believe the different orientations of the allylidene ligands in **2a**,**c** are due to (fortuitous) crystal packing forces. The structural differences between **2a** and **2c** are clearly visible in the superposition of the two structures shown in Figure 6.

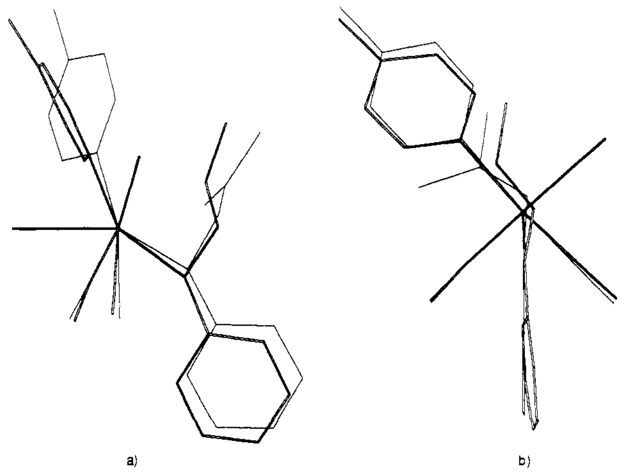
a) b)

Figure 5. Two views of the superimposition of the structures of complexes **2a**,**b**. The structure of complex **2a** is highlighted.

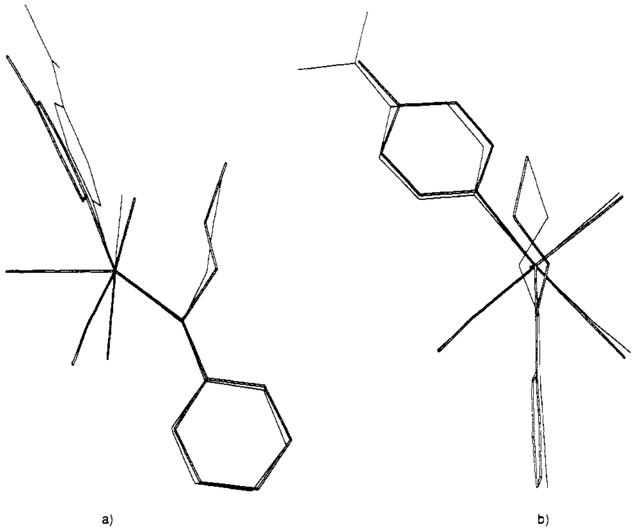
a) b)

Figure 6. Two views of the superimposition of the structures of complexes **2a**,**c**. The structure of complex **2a** is highlighted.

It is of interest here to compare the structures of complexes **2a**–**c** with those of the related tungsten complex W(η^3-CPh-CPhCHTol)(η^5-C$_5$H$_5$)I(CO), **4**, reported by Geoffroy and coworkers.[14j] In this compound the distance between the metal and the alkylidene carbon of 1.999(7) Å is slightly longer than in structures **2a**–**c** and the metal–vinyl distances are distinctly shorter, W–C$_\beta$ = 2.305(8) Å and W–C$_\gamma$ = 2.293(8) Å, falling in the established range of tungsten–allyl bond distances.[22] The

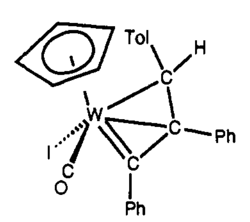

4

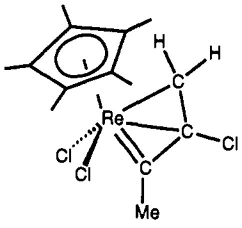

5

near planarity of the vinyl group found in structures **2a–c** is not seen in **4**. The γ-carbon atom of the allylidene ligand in **4** is slightly pyramidalized. The bonding parameters for the allylidene ligand in **4** are more similar to those of other structurally characterized η^3-allylidene complexes, such as the rhenium complex Re(CMeCClCH$_2$)Cl$_2$(η^5-C$_5$Me$_5$), **5**, which was reported by Herrmann and co-workers.[14f,h] The qualitative difference in the bonding of the allylidene ligands in complexes **2** on the one hand and in complexes **4** and **5** on the other hand is evident from a comparison of the bond distances listed in Table VIII. For a detailed comparison of the various types of allylidene complexes, we refer to the discussion by Hofmann.[16]

Description of the Solution Dynamic Behavior of the Allylidene Complexes. The two sets of low-temperature NMR spectra observed for complexes **2a–c** are assigned to two conformational diastereomers I and II with opposite orientations of the vinyl group, as represented by structures **2a,c**. The relative ratio of the two conformers is about 2:1 for both **2a,c**. The most characteristic spectroscopic difference between the isomers I and II is the splitting of the pyridine α-hydrogen signals of the more abundant conformer I into two signals, presumably due to hindered rotation of the pyridine ligands. From the perspective in Figure 6b it may be seen that the vinyl group in **2a** has closer interactions with the picoline ligand than the vinyl group in **2c**. The distance C(17)–N(1) is the closest contact between these ligands in both structures. It is 2.812 Å in **2a** and 3.052 Å in **2c**. Since the shorter contact is likely to inhibit the rotation of the pyridine ligand more strongly, the vinyl group is postulated to adopt the orientation of structure **2a** in the more abundant conformers I. This assignment is supported by the shift of the ^{1}H NMR signal for C(17)H of the more abundant conformer I to higher field: C(17)H in complex **2a** is located in the shielding cone of the picoline ligand.[27] The dynamic process revealed by variable-temperature NMR is proposed to involve the interconversion of the two conformers I and II, which are represented by structures **2a,c**. In structure **2b**, the vinyl group is "stopped" at an intermediate stage. Therefore, the three structures represent three distinct snapshots of the solution dynamic behavior.

The NOE experiments show that the vinyl hydrogen atom C(17)H of **2a** is on average closer to the picoline ligand than the methyl group C(18)H$_3$.[28,29] In the solid-state structure of **2a** the C(17)H–HC(3) distance of 2.51 Å is the shortest contact between hydrogen atoms of the picoline and allylidene ligands. The closest H–H distance between the methyl group C(18)H$_3$ and the picoline ligand, C(18)H–HC(7), is 3.27 Å. Because of the short two-bond connection W–C(9)–C(16) between the metal center and the vinyl group, the side of the vinyl group containing the C(9)–C(16) bond and the C(17)–H bond is tilted toward the metal center and the side containing the C(17)–C(18) bond and the C(16)–H bond is tilted away from the metal center. As a consequence, C(17)–H is pointing toward the picoline α-H atoms while the C(18)H$_3$ group is more remote from the picoline ligand.

Table VIII. Characteristic Bond Distances (Å) of Complexes **2a**, **2b**, **4**, and **5**

complex	M–C$_\alpha$	M–C$_\beta$	M–C$_\gamma$	C$_\alpha$–C$_\beta$	C$_\beta$–C$_\gamma$
2a	1.98(2)	2.38(2)	2.60(2)	1.44(2)	1.35(1)
2b	1.951(8)	2.440(11)	3.158(8)	1.49(2)	1.34(2)
2c	1.987(9)	2.33(1)	2.58(1)	1.48(1)	1.28(1)
4	1.999(7)	2.305(8)	2.293(8)	1.420(1)	1.443(11)
5	1.967(3)	2.242(2)	2.192(3)	1.363(4)	1.410(4)

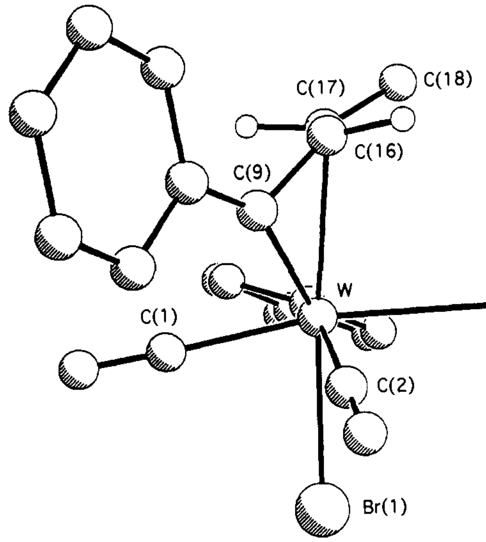

Figure 7. Perspective of the structure of **2a** along the axis connecting the vinyl carbon atoms C(16) and C(17).

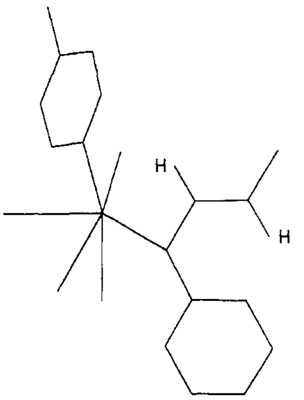

Figure 8. Simulation of the η^1-allylidene conformation of complex **2a**. Except for the vinyl group, the coordinates of structure **2b** were used.

The perspective of **2a** shown in Figure 7 illustrates this situation. The NOE experiments also indicate that the hydrogen atom C(16)H is getting into contact with the picoline α-hydrogen atoms. In the solid-state structure of **2a**, the closest distance between C(16)H and the picoline ligand, C(16)H–HC(7), is 4.86 Å. This distance is probably too far to observe a NOE.[29] However, rotation of the vinyl group about the C(9)–C(16) bond brings C(16)H closer to the picoline ligand. In the transoid conformation of the W=C–C=C system, η^1-**2a**, shown in Figure 8, the approximate C(16)H–HC(3) distance is only 2.3 Å. Rotation of the picoline ligand easily shortens this distance further to 1.5 Å. The transoid conformation of the W=C–C=C system (η^1-vinylcarbene) is probably stabilized by conjugation of the π systems and by a β-agostic interaction between the metal center and the C(16)–H bond.[30] This stabilization of the η^1-configuration could significantly increase the lifetime of the transoid conformation of the metallabutadiene system and thus shorten the time-averaged distance between C(16)H and the picoline α-hydrogen atoms. Another distinct result of the NOE experiments is the absence of enhancement of the phenyl signals upon irradiation at the

---

(27) Johnson, C. E.; Bovey, F. A. *J. Chem. Phys.* **1958**, *29*, 1012.

(28) Internal relaxation of the protons within the methyl group may have reduced the NOE of the methyl group.[29]

(29) (a) Martin, M. L.; Delpuech, J.-J.; Martin, G. J. *Practical NMR Spectroscopy*; Heyden: London, 1980. (b) Noggle, J. H.; Shirmer, R. E. *The Nuclear Overhauser Effect*; Academic Press: New York, 1971.

frequency of the picoline α–H atoms. This observation strongly indicates that the allyidene ligand does not rotate relative to the square pyramidal $WBr_2(CO)_2$(4-pic) fragment. Therefore, in solution the alkylidene carbon atom appears to be locked into the same position relative to the $W(CO)_2$ triangle as found in the solid-state structures.

The combined crystallographic and NMR spectroscopic data lead to the following detailed description of the solution dynamic behavior. The primary motion is the oscillation of the vinyl group about the C(9)–C(16) bond. The extent of rotation, as measured by the difference of the dihedral angles W–C(9)–C(16)–C(17) as structures **2a**,**c**, is approximately 245°. To bring the vinyl group into optimal positions for interaction with the metal center, the C(9)–C(16) bond swivels with each oscillation of the vinyl wing. The swivel angle, as measured by the difference of C(1)–W–C(9)–C(16) for **2a**,**c**, is about 30°. At the turning points the vinyl group is oriented roughly parallel to the adjacent metal ligand bond, i.e. the W–N(1) bond in **2a** or the W–Br(2) bond in **2c**. As the vinyl group departs from the metal center, the adjacent ligand, e.g. N(1), relaxes away from the capping site Br(1), and as the vinyl group approaches the other ligand, e.g. Br(2), that ligand is pushed toward the capping site. The adjustments of the N(1)–W–Br(1) and Br(2)–W–Br(1) bond angles, as measured by the differences between structures **2a**,**c**, are 3.5 and 6.7°, respectively. The superimposition of structures **2a**,**b** in Figure 5a also shows that the carbene carbon moves away from the carbonyl ligands as the metal–vinyl interaction weakens.[31]

Qualitative Bonding Considerations. The bonding of allylidene ligands was recently studied in detail by Hofmann and coworkers.[16] The calculations show that the complexes described in this work most closely mimick the intermediates of the Dötz reaction. Two specific conclusions of the theoretical study, namely weak π back-bonding from the metal to the vinyl group and facile η^3–η^1-interconversion of the allylidene ligands, are fully confirmed by our experimental work.

In the case of the present compounds it may even be argued that π back-bonding from the metal center to the vinyl group is negligible.[8] The six tungsten electrons may be distributed as follows, counting the metal and the ligands all as neutral. Two electrons are used in the bonding of the bromine atoms. Two further electrons are used to form the metal–carbon π bond. The vinyl group lies in or close to the nodal plane of the metal–carbon π bond. Therefore, the vinyl group cannot interact with these electrons. The remaining two electrons are involved in π back-bonding to the carbonyl ligands. To satisfy the π back-bonding requirements of both carbonyl ligands, these electrons neccessarily occupy a d orbital located in the $W(CO)_2$ plane. To utilize these electrons for π back-bonding, the vinyl group would have to be located in the same plane, which is not the case. Consequently, the metal center in complexes **2a**–**c** cannot provide d electrons for π back-bonding to the vinyl group; i.e., the vinyl group is acting as a σ donor ligand only.

The electronic nature of allylidene complex **4** differs markedly from that of complexes **2**. Complex **4** is more electron-rich. It contains only a single carbonyl ligand, and its coordination geometry is different. As a consequence, the conditions for π back-bonding from the metal center are not as restrictive as in complexes **2**.

Complexes **2a**,**c** fit into the category of metal η^3-allylidene complexes, even though the distances between the metal center and the β- and γ-carbon atoms are rather long. In complex **2b**, the γ-carbon atom is not within bonding range of the metal center. Nevertheless, the bonding in all three allylidene complexes **2a**–**c** is qualitatively the same: the vinyl group is donating its π electrons to the metal center. We note, however, that complex **2b** does feature some unusual spectroscopic properties: the carbonyl stretching frequencies are lower than those of both **2a** and **2c** and the chemical shift of the γ-carbon atom is at unusually low field. The origin of these spectroscopic differences is not entirely clear, but the dimethylvinyl group is most likely a stronger donor group, giving rise to lower carbonyl stretching frequencies, and the interaction of the metal center with the electrophilic metal center with C(2) could confer some carbocationic character to C(3), causing a shift of the ^{13}C NMR signal to lower field.

Because of the negligible conjugation between the metal–carbon double bond and the carbon–carbon double bond, the vinyl groups in complexes **2** may be considered as alkene ligands which "happen" to be covalently connected. By virtue of their particular electronic properties complexes **2** are therefore unique examples of transition metal alkene complexes in which the otherwise omnipresent π back-bonding component is "turned off". It seems appropriate to conclude from the NMR spectroscopic and X-ray crystallographic results, which reveal very weak metal–vinyl interactions in complexes **2a**–**c**, that transition metal alkene complexes without a significant π back-bonding component would be very labile. This is in agreement with the generally accepted bonding concepts for transition metal alkene complexes.[32]

There must be electronic reasons for the "fixed" location of the alkylidene carbon atom relative to the metal–dicarbonyl triangle, since no obvious restrictive steric interactions between the square pyramidal metal complex fragment and the allylidene ligand exist. As pointed out above, the carbonyl π* orbitals in the $W(CO)_2$ plane interact with a filled metal d orbital. The out-of-plane carbonyl π* orbitals are in a position to interact with the metal–carbon π system of the carbene ligand. The out-of-phase combination of these carbonyl π* orbitals has the same symmetry as the bonding combination of the metal–carbene π orbital. Interaction of these orbitals could account for the "interlocking" of the two carbonyl ligands and the alkylidene ligand. Incipient bonding between ligands in other seven-coordinate complexes has previously been noted by Hoffmann et al.[33]

The mechanism of the dithiocarbamate-induced coupling of vinylcarbene and carbonyl ligands in **2a** was investigated in some detail.[18] That work shows that the close contacts between the alkylidene carbon atom and the carbonyl carbon atoms in **2a** have no direct bearing on the coupling process.

Experimental Section

All operations were carried out under an atmosphere of N_2 using Schlenk techniques. The solvents CH_2Cl_2 (P_2O_5 or CaH_2), ether (Na/benzophenone), and hexane (CaH_2) were dried and distilled prior to use. Elemental analyses were performed by Schwarzkopf Analytical Laboratory.

[W(CPh)Br(CO)$_2$(NC$_5$H$_4$Me-4)$_2$], 1a.[34] A cold (−78 °C) solution of oxalyl bromide (1 equiv) in CH_2Cl_2 (5 mL/mmol) is added to a cold (−78 °C) solution of $NMe_4[W(COPh)(CO)_5]$[35] in CH_2Cl_2 (15 mL/mmol). The resulting dark orange solution is warmed to −10 °C wherby the color turns yellow. At that point 4-picoline (5 equiv) is added, and the solution is warmed to 40 °C and stirred for 2 h, whereby the evolving CO is allowed to escape. The solvent is removed from the resulting dark brown solution and the residue washed with hexane. The product is purified by recrystallization from CH_2Cl_2/ether to give orange crystals (yield ranging 60–90%). IR (CH_2Cl_2, cm^{-1}): ν(CO) 1987 (s), 1898 (s). ^1H NMR ($CDCl_3$): δ 8.89 (d, 4H, $J = 6.47$ Hz, pic α–H), 7.31–7.21 (m, 5H, Ph), 7.06 (d, 4H, $J = 6.12$ Hz, pic β–H), 2.34 (s, 6H, CH_3).

[W(CPh)Br(CO)$_2$(NC$_5$H$_4$NMe$_2$-4)$_2$], 1b. The solutions of $NMe_4[W(COPh)(CO)_5]$ (0.502 g, 0.84 mmol) (40 mL of CH_2Cl_2) and oxalyl

---

[30] Feng, S. G.; White, P. S.; Templeton, J. L. *J. Am. Chem. Soc.* **1992**, *114*, 2951.

[31] Of course, conclusions regarding the solution dynamic behavior on the basis of small structural changes, especially if only a set of a few solid-state structures is available, need to be considered with caution: Bürgi, H.-B. *Angew. Chem.* **1975**, *87*, 461; *Angew. Chem., Int. Ed. Engl.* **1975**, *14*, 460.

[32] (a) Dewar, M. J. S. *Bull. Soc. Chim. Fr.* **1951**, *18*, C79. (b) Chatt, J.; Duncanson, L. A. *J. Chem. Soc.* **1953**, 2339. (c) Albright, T. A.; Hoffmann, R.; Thibeault, J. C.; Thorn, D. L. *J. Am. Chem. Soc.* **1979**, *101*, 3801.

[33] Hoffmann, R.; Beier, B. F.; Muetterties, E. L.; Rossi, A. R. *Inorg. Chem.* **1977**, *16*, 511.

[34] Filippou, A. C.; Grünleitner, W. Z. *Naturforsch., B* **1989**, *44*, 1023.

[35] Fischer, E. O.; Maasböl, A. *Chem. Ber.* **1967**, *100*, 2445.

bromide (0.079 mL, 0.84 mmol) (10 mL of CH_2Cl_2) are cooled to −78 °C. Then the oxalyl bromide solution is added to the solution of the tungsten acyl complex. The resulting dark orange solution is warmed to 0 °C whereby the color turns lighter. After addition of 4-(dimethylamino)pyridine (0.206 g, 1.67 mmol) the solution is warmed to room temperature and stirred for 2 h, whereby the evolving CO is allowed to escape. The solvent is removed from the resulting dark brown solution and the residue washed with hexane. The product is purified by filtration of a methylene chloride solution through a plug of silical gel at −78 °C and recrystallization from CH_2Cl_2/ether to give orange-red crystals (0.313 g, 57%). IR (CH_2Cl_2, cm^{-1}): ν(CO) 1979 (s), 1887 (s), ν(NC_5H_4–NMe_2) 1621 (m), 1537 (w). ^1H NMR (CD_2Cl_2): δ 8.42 (d, 4H, ^3J = 7.05 Hz, pyridine α–H), 7.99–7.17 (m, 5H, C_6H_5), 6.33 (d, 4H, ^3J = 7.11 Hz, pyridine β–H), 2.93 (s, 6H, $N(CH_3)_2$). ^{13}C NMR (CD_2Cl_2): δ 263.3 (CPh), 223.2 (CO), 154.6, 152.8 (pyridine), 139.0, 129.1, 128.2, 127.3 (Ph) 107.0 (pyridine), 39.3 ($N(CH_3)_2$). Anal. Calcd for $C_{23}H_{25}BrN_4O_2W$ (MW = 653.229): C, 42.29; H, 3.86. Found: C, 42.58, H 3.68.

[W(CPhCHCHMe)$Br_2(CO)_2$(4-pic)], 2a. A solution of 1.003 g of **1a** and 1.5 mL of allyl bromide in 25 mL of CH_2Cl_2 is warmed to 40 °C for 1.5 h. During this time the color of the solution turned from bright orange to dark orange brown. Then all volatiles are removed in vacuo. The product is chromatographed at −10 °C on a silica gel column (2 × 20 cm) using CH_2Cl_2 as the eluant. Recrystallization from CH_2Cl_2/pentane provides dark brown crystals (0.434 g, 0.67 mmol, 40%). IR (CH_2Cl_2, cm^{-1}): ν(CO) 2025 (m), 1944 (s). ^1H NMR ($CDCl_3$), 297 K: δ 9.09 (m, 2H, pic α–H), 7.75–7.79 (m, 2H, Ph), 7.47–7.52 (m, 3H, Ph), 7.26–7.29 (m, 2H, pic β–H), 5.55–5.67 (m, 1H, C*H*Me), 5.29 (d, 1H, ^3J = 11.67Hz, CH), 2.47 (s, 3H, pic CH_3), 1.86 (d, 3H, ^3J = 6.11 Hz, vinyl CH_3). ^1H NMR ($CDCl_3$), 211 K (two isomers, I and II, relative ratio 2:1): δ 9.72 (br m, 1H, pic α–H, I), 8.76 (d, 2H, J = 6.28 Hz, pic α–H, II), 8.60 (br m, 1H, pic α–H), 7.81–7.76, 7.55–7.47, 7.24–7.22 (m, 14H for I and for II, Ph and pic β–H), 5.78–5.66 (m, 1H, CHMe, II), 5.50–5.39 (m, 1H, CHMe, I), 5.27 (d, 1H, ^3J = 11.51 Hz, CH, I), 5.21 (d, 1H, ^3J = 11.43 Hz, CH, II), 2.50 (s, 3H, pic CH_3, I), 2.43 (s, 3H, pic CH_3, II), 1.85 (d, vinyl CH_3, II), 1.81 (d, 3H, ^3J = 6.10 Hz, vinyl CH_3, I). Estimated coalescence temperatures: signals at 5.27 and 5.21, 248 K; signals at 2.50 and 2.43; 243 K; signals at 1.85 and 1.81, 243 K. NOE difference experiments (CD_2Cl_2) at 221 K indicate that irradiation at the resonance frequency of the picoline α–H atoms results in significant enhancement of the following signals: picoline β–H and vinyl CHMe. Very small enhancements are observed for the vinyl CH and vinyl CH_3 atoms. Irradiation at the resonance freqency of the vinyl CHMe atom results in significant enhancement of the picoline α–H atoms. Minor enhancements are observed for the phenyl *o*–H atoms and the vinyl CH and vinyl CH_3 atoms. ^{13}C NMR (CD_2Cl_2), 293 K: δ 240.3 (CPh), 210.8, 209.8 (CO), 153.7 (d), 152.6 (s), 140.1 (s), 133.1 (d), 132.6 (d), 129.8 (d), 127.3 (d) (pic and Ph), 122.9 (d, J_{CH} = 161.5 Hz, CHMe), 91.3 (d, J_{CH} = 165.1 Hz, CH), 21.4 (q, pic CH_3), 17.2 (q, vinyl CH_3).

[W(CPhCHCMe_2)$Br_2(CO)_2$(4-pic)], 2b. A solution of 1.014 g (1.70 mmol) of **1** and 1.05 g (7.77 mmol) of 2-methylallyl bromide in 30 mL of CH_2Cl_2 is warmed to 40 °C for 2.75 h. Completion of the reaction is assured by IR. The solvent is removed in vacuo. The residue is redissolved in CH_2Cl_2 and chromatographed on silica gel (13 × 2.5 cm) using CH_2Cl_2 as the eluant. A dark brown band is collected (75 mL). The volume of the solution is reduced to 5 mL. Then 20 mL of ether is added slowly to give a precipitate. The volume is again reduced to about 5 mL, and 20 mL of pentane is added. Then 5 mL of solvent is removed, the solid is allowed to settle, and the supernatant is decanted. The residue is dried in vacuo. Crude yield: 0.634 g (0.995 mmol, 58.4%). The product is further purified by a second chromatography on silica gel (14 × 1 cm) using CH_2Cl_2 as the eluant. The collected solution is reduced to about 3 mL and transferred into a test tube, which is placed in a 250-mL Schlenk flask containing 150 mL of ether. After 1 week the cloudy supernatant is decanted from brown crystals, which are washed with ether and dried in vacuo. Yield: 0.193 g (0.307 mmol, 18%). IR (CH_2Cl_2, cm^{-1}): ν(CO) 2007 m, 1923 s. ^1H NMR ($CDCl_3$), 327 K: δ 9.13 (d, 2H, J = 5.86, pic α–H), 7.54–7.34 (m, 5H, Ph), 7.27 (d, 2H, J = 6.16 Hz, pic β–H), 5.65 (br s, 1H, CH), 2.46 (s, 3H, pic CH_3), 1.81 (d, 3H, J = 0.84 Hz, vinyl CH_3), 1.62 (bs, 3H, vinyl CH_3). ^1H NMR ($CDCl_3$) 211 K (two isomers, I and II, relative ratio 1.1:1, peak assignments to individual isomers somewhat uncertain): δ 9.28 (bs, 2H, pic α–H, I), 8.84 (d, ^3J = 6.15 Hz, pic α–H, II), 7.73–7.28 (m, Ph and pic β–H), 6.07 (s, 1H, CH, I), 5.21 (s, 1H, CH, II), 2.48 (s, 3H, pic CH_3, I), 2.44 (s, 3H, pic CH_3, II), 2.03 (s, 3H, vinyl CH_3, II), 1.95 (s, 3H, vinyl CH_3, II), 1.80 (s, 3H, vinyl CH_3, I), 1.10 (s, 3H, vinyl CH_3, I). Estimated coalescence temperatures: signals at δ 9.28 and 8.84, 276 K; 6.07 and 5.21, 278 K; 2.48 and 2.44, 255 K; 1.95 and 1.80, 270 K; 2.03 and 1.10, 281 K. ^{13}C NMR (CD_2Cl_2), 305 K: δ 230 (br, CPh), 213.9, 212.6 (CO), 153.9, 153.1, 142.5, 133.7, 131.2, 129.8, 127.1 (Ph and pic), 91.9 (br, vinyl CH), 32.4 and 27.5 (vinyl CH_3), 21.6 (pic CH_3), (signal for CMe_2 not found). ^{13}C NMR (CD_2Cl_2), 231 K (two isomers, I and II, approximate relative ratio 1.6:1): δ 233.3 (s, CPh, II), 230.0 (s, CPh, I), 214.2 (s, CO, II), 212.5 (s, J_{WC} = 142.3 Hz, I), 212.4 (s, J_{WC} = 158.0 Hz, CO, I), 212.0 (s, CO, II), 204.8 (s, CMe_2, II), 194.5 (s, CMe_2, I), 153.9 (d, J_{CH} = 181.8 Hz), 153.0 (s), 152.5 (d, J_{CH} = 178.9 Hz), 141.5 (s), 141.1 (s), 133.6 (d, J_{CH} = 162.2 Hz), 133.2 (d, J_{CH} = 159.7 Hz), 130.8 (d, J_{CH} = 144.9 Hz), 129.3 (d, J_{CH} = 161.5 Hz), 126.8 (d, J_{CH} = 159.0 Hz), 126.6 (d, J_{CH} = 173.9 Hz) (pic and Ph), 92.9 (d, J_{CH} = 167.0 Hz, vinyl CH, I), 86.9 (d, J_{CH} = 161.6 Hz, vinyl CH, II), 32.9 (q, J_{CH} = 129.0 Hz, II), 31.9 (q, J_{CH} = 128.4 Hz, I), 28.0 (q, J_{CH} = 126.7 Hz, II), 25.6 (q, J_{CH} = 131.0 Hz, I) (vinyl CH_3), 21.3 (q, J_{CH} = 129.8 Hz, pic CH_3, I and II).

[W(CPhCHCHMe)$Br_2(CO)_2$($NC_5H_4NMe_2$-4)], 2c. A solution of 0.95 g (1.5 mmol) of **1b** and 1.31 mL (15 mmol) of allyl bromide in CH_2Cl_2 (50 mL) is warmed to 40 °C for 2 h. Then the solvent is removed in vacuo to give a brown oil, which is washed twice with hexane. The residue is redissolved in a small amount of CH_2Cl_2 and transferred to a silica gel column (10 × 2 cm). The product is eluted with CH_2Cl_2 as a brown band. The solvent is removed from the collected fraction, and the solid is recrystallized from CH_2Cl_2/hexane to give dark-brown crystals (0.27 g, 28%). IR (CH_2Cl_2, cm^{-1}): ν(CO) 2024 (m), 1938 (s), ν(NC_5H_4–NMe_2) 1625 (m), 1541 (w). ^1H NMR (CD_2Cl_2), 287 K: δ 8.63 (br d, 2H, pyridine α–H), 7.75–7.66 (m, 2H, C_6H_5), 7.48–7.42 (m, 3H, C_6H_5), 6.49 (d, 2H, pyridine β–H), 5.87–5.22 (m, 1H, CHMe), 5.23 (d, 1H, ^3J = 12.09 Hz, CH), 3.02 (s, 6H, $N(CH_3)_2$), 1.76 (d, 3H, ^3J = 6.29 Hz, CH_3). ^1H NMR (CD_2Cl_2), 232 K (two isomers, I and II, approximate relative ratio 2:1): δ 9.21 (d, 1H, pyridine α–H, I), 8.38 (d, 2H, pyridine α–H, II), 8.30 (d, 1H, pyridine α–H, I), 7.79 (m) and 7.55 (br s) (Ph), 6.66 (br d, 1H, pyridine β–H, I), 6.55 (br, 1H, pyridine β–H, I), 6.46 (d, 2H, pyridine β–H, II), 5.89 (m, 1H, CHMe, II), 5.71 (m, 1H, CHMe, I), 4.73 (d, 1H, CH, II), 4.71 (d, 1H, CH I), 2.59 (s, 6H, $N(CH_3)_2$, I), 2.56 (s, 6H, $N(CH_3)_2$, II), 1.80 (d, 3H, CH_3, II), 1.78 (d, 3H, CH_3, I). ^{13}C NMR (CD_2Cl_2), 293 K: δ 210.7 (CO), 210.0 (CO), 155.1, 153.0 (pyridine), 140.3, 133.0, 132.1, 130.7, 129.7, 126.1 (Ph), 120.9 (CHMe), 108.4 (pyridine), 89.6 (vinyl CH), 39.5 ($N(CH_3)_2$), 17.3 (vinyl CH_3). Due to low solubility, the alkylidene carbon was not observed and the carbonyl resonances were barely visible. During measurement of the spectrum (8 h at room temperature) the sample partially decomposed. Anal. Calcd for $C_{19}H_{20}Br_2N_2O_2W$ (MW = 652.036): C, 35.00; H, 3.09. Found: C, 35.38; H, 3.07.

Structure Determination for 2a. Crystal data are collected in Table I. The intensity measurements were made at −93 ± 3 °C, using graphite-monochromated Mo Kα radiation and a variable-rate, ω-scan technique. Empirical absorption corrections were applied on the basis of azimuthal scans of suitable reflections. Data with $[|F_o| \geq 3\sigma(F_o)]$ were considered observed. The structure was solved (SHELXTL software) by conventional heavy-atom methods. All hydrogen positions were located on difference Fourier maps following refinement of the non-hydrogen atoms. The phenyl and methyl hydrogen positions were subsequently idealized with C–H = 0.96 Å and B(H) = 1.2*B*(C). In the final cycles of blocked-cascade least-squares refinement, all non-hydrogen atoms were refined with anisotropic temperature factors, H(16) and H(17) were held fixed, and a riding model was used for the remainder of the hydrogen atoms. Final refinement with 217 parameters converged at R = 0.036 and R_w = 0.037 with goodness of fit = 1.25.

Structure Determination for 2b. Crystal data are collected in Table I. A single crystal of $C_{19}H_{19}Br_2NO_2W$ measuring 0.15 mm × 0.25 mm × 0.35 mm was mounted on a glass fiber and centered on a Nicolet R3m diffractometer. Cell constants and their esd's were determined by a least-squares fit of 23 diffractometer-measured reflections with 20° ≤ 2θ ≤ 25°. All intensity measurements were made at room temperature. Background counts were taken for half the scan time at each extreme of the scan range. All data (4356) having $k, l \geq 0$ with 3° ≤ 2θ ≤ 52° were measured in this manner. Crystal decomposition was monitored throughout data collection by remeasuring two standard reflections after every 50 data measurements; no significant variations in intensity were observed. The intensities were reduced by applying Lorentz, polarization, and empirical absorption corrections. Systematically absent reflections were eliminated and equivalent reflections were averaged to give 4048 unique data of which 2991 were considered to be observed $[|F_o| > 3\sigma(F_o)]$.

The structure was solved (SHELXTL software) by conventional heavy-atom techniques. Following refinement of the non-hydrogen atoms with anisotropic temperature factors, difference Fourier maps displayed peaks at plausible positions for all hydrogens except H(2). The located hydrogen atoms were subsequently entered at idealized positions (C–H = 0.96 Å; CCH = 109 or 120°) and were varied using a riding model. H(2) was not included in refinement. Refinement converged (shift/error ≤ 0.10) at $R = 0.051$ and $R_w = 0.039$. The largest peaks in a final difference map (maximum e/Å^3 = 1.35) were in the vicinity of the tungsten atom.

Structure Determination for 2c. Crystal data are collected in Table I. An Enraf-Nonius CAD4 diffractometer was used for data collection and unit cell measurements. Crystals were grown from CH_2Cl_2/pentane. A suitable crystal (0.3 × 0.3 × 0.1 mm) was found and mounted on the tip of a thin glass fiber with epoxy glue. After the mounted crystal was centered in the X-ray beam, 25 reflections were located by an automatic search program. The unit cell was triclinic with space group $P\bar{1}$ (No. 2). Data were collected at ambient temperature from $0 < 2\theta < 60.8$. The structure was solved using the Texsan structure determination package. The tungsten atom was located on a Patterson map, and other non-hydrogen atoms were located on subsequent difference Fourier maps. The hydrogen atom positions were calculated, and the non-hydrogen atoms were refined anisotropically, resulting in a final R value of 0.044 and R_w of 0.039 using 3123 observed reflections ($I > 3\sigma$).

Acknowledgment. We thank Michael Rickenbach and Prof. Stephen A. Koch for solving the solid-state structure complex **2c**, Diana Keupp for growing crystals of **2c**, and Richard T. Chang and Tsung-Yi Lee for doing the NMR measurements on **2c**. Support for this work by the donors of the Petroleum Research Fund, administered by the American Chemical Society, and by the National Science Foundation is gratefully acknowledged.

Supplementary Material Available: For **2b**,**c**, Tables of positional and thermal parameters, bond lengths, and bond angles (6 pages); tables of observed and calculated structure factors (40 pages). Ordering information is given on any current masthead page. Supplementary material regarding the structure determination of complex **2a** is given in ref 7.